

The Mpemba effect likes to hit a wall

Yue Liu,¹ Tan Van Vu,¹ Raphaël Chétrite,² Frédéric van Wijland,^{3,1} and Hisao Hayakawa¹

¹*Center for Gravitational Physics and Quantum Information,
Yukawa Institute for Theoretical Physics, Kyoto University,
Kitashirakawa Oiwakecho, Sakyo-ku, Kyoto 606-8502, Japan*

²*Institut de Physique de Nice (INPHYNI), Université Côte d'Azur &
CNRS (UMR 7010), 17 rue Julien Lauprêtre, 06200, Nice, France*

³*Laboratoire Matière et Systèmes Complexes (MSC),
Université Paris Cité & CNRS (UMR 7057), 75013 Paris, France*

The historical Mpemba effect involves a first-order phase transition. This has prompted the experimental realization of microscopic proxies in the form of a colloidal particle trapped in an asymmetric double well, for which the Mpemba effect has indeed been observed. We establish that the existence of the one-dimensional Mpemba effect for a polynomial potential is driven solely by the presence of a hard enough boundary, irrespective of the potential's double-well shape. We then show that the physics of the underlying Mpemba effect is governed not only by single-well physics but also by the high-temperature initial regime.

Since the seminal report by Mpemba and Osborne [1], it has been recognized that a system initially prepared at a higher temperature may relax to equilibrium faster than one prepared at a lower temperature when both are quenched into a cold bath. This counterintuitive phenomenon, now broadly referred to as the Mpemba effect, has become a paradigmatic example of anomalous relaxation. While its existence in macroscopic systems, often phrased as faster freezing from hotter initial conditions, remains under active debate [2, 3], compelling experimental evidence has established its presence in controlled settings. In particular, the experiment of Ref. [4], involving a colloidal particle in a tunable one-dimensional (1D) optical potential, demonstrated such anomalous relaxation by varying the initial bath temperature. These findings have stimulated extensive investigations of the Mpemba effect across a wide range of systems, spanning colloidal [4–8], classical [9–31], and quantum regimes [32–51].

The idea of Ref. [9], experimentally investigated in [4, 52], is to use a double-well potential to mimic the metastability underlying a macroscopic first-order transition. We will also restrict our analysis to that particular setting, reserving the case of more general 1D potentials (symmetric, single well, with or without walls) to a longer version [53]. Although the most recent works on the Mpemba effect address nonequilibrium initial conditions [10, 13–18, 23, 32–51], we choose to focus on the original setup in which we compare the dynamics from two initial equilibrium conditions at different temperatures [1, 4–9, 11, 12, 19, 21, 22, 25–30, 52].

The physical gist of a double-well potential is to introduce a timescale (which can be made arbitrarily large as the bath temperature is lowered) during which the anomalous relaxation effect of interest can be properly observed. For our physical discussion, we consider 1D double-well potentials confined by two hard walls, which can be taken to infinity. Many of the references we cite

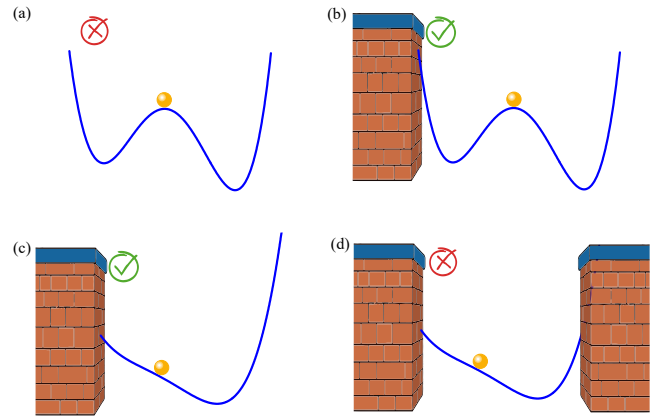


FIG. 1. The presence (✓) or absence (✗) of the Mpemba effect is shown for an asymmetric potential with a right wall far away (a,b,c) and close enough (d). If the left wall (absent in (a)) is located far away, in units of the distance to the wall, the inner structure of the potential is shrunk, and the effective (b) potential looks like (c). The inner structure of the potential plays no role in the Mpemba effect itself.

address this setting [5, 7, 19, 54], each emphasizing different physical mechanisms underlying anomalous relaxation, including the role of the energy barrier separating the two potential wells. These works adopt various realizations, ranging from smooth to sawtooth or square double-well potentials. However, mutual comparison is often cumbersome, simply because the parameter space to explore, location of the wells, widths, curvatures, well depths, barrier height, slopes, is huge. Our work rationalizes these various physical ingredients.

In this work, we argue that the primary physical mechanism driving the existence of an Mpemba effect for an arbitrary double-well polynomial potential in 1D has not been identified hitherto. In our analysis, the 1D Mpemba effect is an artifact of the presence of a wall on the shallow

side, and it simply disappears in its absence, regardless of the shape of the double-well potential and the presence of a wall on the deep side. In what follows we shall resort to a hard-wall picture, though, as will appear from our argument, a steeper potential break is good enough of a wall. A wall is a necessary condition but not sufficient (as it can be suppressed by an appropriately located wall on the deep side). We begin by showing that when the bath temperature is low, the Mpemba effect appears when a boundary is included, and that the corresponding mechanisms are rooted in the equilibrium thermal properties of an effective single-well potential. We then fill in the intermediate range of initial and final temperatures with numerical simulations. We synthesize our findings by proposing a mechanism based on a detailed analysis of the response of the initial equilibrium population with respect to a temperature change. Our findings are summarized in the cartoon of Fig. 1.

The general setting of our study is a 1D overdamped Langevin equation describing a particle with position $x(t)$ evolving in a potential landscape $V(x)$ with a unit mobility:

$$\frac{dx(t)}{dt} := -V'(x(t)) + \sqrt{2T}\eta, \quad (1)$$

where η is a zero average Gaussian white noise with correlations $\langle \eta(t)\eta(t') \rangle = \delta(t-t')$, $T = \beta^{-1}$ is the bath temperature (k_B is set to unity), and the potential V becomes infinity at $x = -L_-$ and $x = L_+$. The Fokker-Planck evolution equation for the probability density $p(x, t)$ to find the particle at position x at time t reads

$$\partial_t p = \mathbb{W}p = \partial_x(V'p) + T\partial_x^2 p. \quad (2)$$

For an initial condition $p(x, 0)$, the solution at time t is obtained as

$$p(x, t) = \sum_{n \geq 1} e^{-\lambda_n t} a_n r_n(x), \quad (3)$$

where $\{\lambda_n\}_{n \geq 1}$ are the non-negative eigenvalues of $-\mathbb{W}$ in ascending order, and $\{r_n\}_{n \geq 1}$ are the corresponding right eigenvectors. The coefficient a_n is obtained by projecting the eigenvector ℓ_n of \mathbb{W}^\dagger onto the initial state,

$$a_n := \int dx \ell_n(x) p(x, 0). \quad (4)$$

Because the dynamics Eq. (1) satisfies the detailed balance property with respect to the Boltzmann distribution $\pi(x, \beta) := e^{-\beta V(x)}/Z(\beta)$ with $Z(\beta) := \int dx e^{-\beta V(x)}$, $p(x, t)$ converges to $\pi(x, \beta)$ at large times. In our study, the system is initially prepared in equilibrium at a temperature $T_i = \beta_i^{-1}$, so that the coefficients a_n depend on T_i in addition to T and $V(x)$. While the lowest eigenvalue $\lambda_1 = 0$ is known ($\ell_1(x) = 1$, $r_1(x) = \pi(x, \beta)$), the specifics of the spectrum are of course heavily potential-dependent [7, 19, 55, 56], up to some robust properties. One of them is that at low bath temperature T ,

$\lambda_2 \propto e^{-\beta \Delta V}$ in accordance with the Arrhenius law, as demonstrated by Kramers [57, 58] (where ΔV is the potential barrier from the least stable well). The corresponding timescale can be made arbitrarily large, leaving ample room to define a quasi-stationary regime in which the Mpemba effect is more readily observed. In the $\lambda_2^{-1} \gg t \gg \lambda_3^{-1}$ regime, we can approximate

$$p(x, t) \simeq \pi(x, \beta) + e^{-\lambda_2 t} a_2 r_2(x) + O(e^{-\lambda_3 t}), \quad (5)$$

which we can use to determine how far $p(x, t)$ lies from $\pi(x, \beta)$. For instance, the authors in Refs. [4, 9] resorted to the Kullback-Leibler divergence $D(p||\pi)(t) = \int dx p(x, t) \ln[p(x, t)/\pi(x, \beta)]$ (or to the L^1 distance). At large times, $D(t) \simeq e^{-\lambda_2 t} a_2 \int dx r_2(x)$, and we see that the whole T_i -dependence is contained in a_2 . Other definitions involve mean first-passage times [59]. We follow the existing literature to define the existence of a Mpemba effect by a non-monotonicity of a_2 as a function of T_i . We will, thus, focus on the existence of a temperature $T_{\mathcal{M}}$ such that $\partial a_2 / \partial \beta_i$ vanishes. The temperature $T_{\mathcal{M}}$ signals the transition between the increase and the decrease of a_2 . This concludes our review of the state of the art. We now turn to an analytical study on the T_i -dependence of a_2 .

Since we sit in a regime where the bath temperature is low, up to an overall prefactor, we can approximate $\ell_2(x)$ by means of the following expression [60, 61]:

$$\ell_2(x) \simeq \frac{1 - e^{-\beta \Delta V}}{2} - \frac{1 + e^{-\beta \Delta V}}{2} \operatorname{erf} \left[\sqrt{\frac{\beta |V''(x^*)|}{2}} (x - x^*) \right], \quad (6)$$

where x^* denotes the position of the barrier top, and $\Delta V > 0$ denotes the energy difference between the two wells. For our discussion, we introduce a boundary located at $x = -L_- (< 0)$ to the left and one at $x = L_+$. In the low temperature limit, $\ell_2(x)$ is basically a step function $\theta(x^* - x)$. Besides, the derivative $\partial a_2 / \partial \beta_i$ has a simple thermodynamic interpretation:

$$\frac{\partial a_2}{\partial \beta_i} = \langle \ell_2(x) (U_i - V(x)) \rangle_{\beta_i}, \quad (7)$$

where the brackets with β_i refer to an equilibrium average with respect to $\pi(x, \beta_i)$, and $U_i = \int dx V(x) \pi(x, \beta_i)$ is the internal energy at temperature T_i .

We analyze a system with a bistable potential $V(x)$, where the two minima of $V(x)$ are located at x_1 and x_2 satisfying $V(x_1) < V(x_2)$ for $x_2 > x_1$. We now establish that a_2 is a monotonic function of β_i when $L_- = +\infty$, but that, for a large yet finite $L_- < L_+$, it possesses an extremum as a function of β_i . Due to Eq. (7), the probabilistic interpretation of the Mpemba condition $\partial a_2 / \partial \beta_i = 0$ is that $V(x(t))$ and $\ell_2(x(t))$ are independent in the initial equilibrium. Physically, this means that the internal energies are equal conditioned to each domain. Indeed, denoting by $p_- := \int_{-L_-}^{x^*} dx \pi(x, \beta_i)$

and $p_+ := \int_{x^*}^{L_+} dx \pi(x, \beta_i)$, we see that Eq. (7) amounts to

$$\underbrace{\frac{1}{p_-} \int_{-L_-}^{x^*} dx V(x) \pi(x, \beta_i)}_{U_-} = \underbrace{\frac{1}{p_+} \int_{x^*}^{L_+} dx V(x) \pi(x, \beta_i)}_{U_+}, \quad (8)$$

and it is now a matter of understanding the behavior of the β_i on each side. To be concrete, we use a fully generic confining polynomial potential that grows as x^n for $|x| \gg 1$ with the form $V(x) = (x-x^*)^n + \sum_{k=0}^{n-1} v_k (x-x^*)^k$ with even n (with the v_k 's adjusted to comply with the asymmetric double well shape). We anticipate that, at the transition, the β_i regime of interest is the high-temperature regime. Preparing for that regime, we write

$$Z(\beta_i) p_- = \beta_i^{-1/n} \int_{-\infty}^0 dx e^{-x^n} e^{-\sum_{k=0}^{n-1} \beta_i^{1-\frac{n}{k}} v_k x^k} - \int_{-\infty}^{-L_-} dx e^{-\beta_i V(x)}, \quad (9)$$

and similar expressions are used not only for the right side but also for the numerators in Eq. (8), which, after some tedious manipulations, lead to

$$U_- = \frac{1}{n\beta_i} + \frac{\sum_{k=0}^{n-1} (n-k)v_k \int_{-L_- - x^*}^0 x^k e^{-\beta_i V(x+x^*)} dx}{nZ(\beta_i)p_-} - \frac{(L_- + x^*)e^{-\beta_i V(-L_-)}}{n\beta_i Z(\beta_i)p_-}, \quad (10)$$

and again, a similar expression holds for U_+ . For both L_- and L_+ large the condition Eq. (8) then leads to $\beta_i = \beta_{\mathcal{M}}$ with the transition temperature given by

$$\beta_{\mathcal{M}} \simeq \frac{C_1 \ln(C_2 L_-)}{L_-^n} + \frac{1}{L_-^n} \ln \left(1 - \frac{L_+}{L_-} e^{-\beta_{\mathcal{M}}(L_+^n - L_-^n)} \right) \quad (11)$$

where C_1 and C_2 are constants. This inverse temperature indeed exists if L_+ is large enough with respect to L_- . Upon sending the right wall to infinity we arrive at

$$\beta_{\mathcal{M}} \propto \frac{\ln L_-}{L_-^n}. \quad (12)$$

The constant C_2 appearing in Eq. (11) arises from the asymmetry of the largest-order odd moment of V on either side of x^* . Note that, for large L_- , the inner structure of the potential plays a minor role; hence, the effective one-well picture of Fig. 1. The details are provided in the End Matter.

Several comments are in order. First, we see from Eq. (12) that, in the absence of a right wall, sending the left boundary to infinity suppresses any possibility of the Mpemba effect since $\beta_{\mathcal{M}} \rightarrow 0$. This establishes

that a boundary on the shallow side is a necessary condition. However, for the effect to occur, we also need an asymmetry that ensures the presence of an odd contribution. Somewhat paradoxically, the initial temperature regime we are studying in Eq. (12) is effectively a low-temperature regime on the left-hand side, since $\beta_{\mathcal{M}} V(-L_-) \sim \ln L_- \gg 1$, in spite of having $T_{\mathcal{M}} \rightarrow +\infty$. In addition, as shown in Eq. (11), if a wall is included on the deep side, provided it is sufficiently far away, it plays no significant role. Nevertheless, bringing the right wall too close eliminates the Mpemba effect as inferred from Eq. (11).

These analytical results establish a condition for the Mpemba effect in the low-bath-temperature regime. The finite-bath-temperature corrections decay exponentially with β , so we expect our results to hold well beyond the zero-temperature limit. We have also used a boundary located far from the left well, which leads to a transition temperature that increases with L_- . Whether the high β and large L_{\pm} results we have obtained are observed in practice for finite values of these parameters is now explored numerically.

We discretize the horizontal axis into $N = 10^4$ lattice points, with the total length, in practice, $[-L_-, L_+]$. We choose L_+ sufficiently large (in agreement with the existence of $\beta_{\mathcal{M}}$ in Eq. (11)) so that our results are independent of L_+ . The evolution operator \mathbb{W} in Eq. (2) is then represented as an $N \times N$ matrix. The latter is diagonalized using the `scipy.linalg` package optimized to search for the first nonzero eigenvalue $\lambda_2(x)$ and eigenvector $l_2(x)$. Then a_2 is determined according to Eq. (4) and the transition temperature $\beta_{\mathcal{M}}$ is then determined from the extremum of a_2 , if it exists. For concreteness, we use a quartic potential of the form $V(x) = (x^2 - 1)^2 - 0.2x$ and a sextic potential of the form $V(x) = (x^2 - 1)^2(x^2 + 1) - 0.2x$ (see the End Matter for another potential). The results for the transition temperature $\beta_{\mathcal{M}}$ as a function of L_-

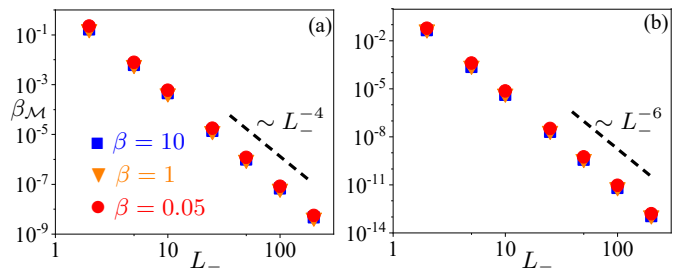


FIG. 2. The inverse temperature $\beta_{\mathcal{M}}$ is shown as a function of L_- for various bath temperatures in a quartic (left) and a sextic (right) potential. The analytical result obtained for large β and L_- is shown as a dashed line for guidance. No notable deviations are observed, even very far from the regime in which the analytical expression was derived. We have used $L_+ = 2L_-$.

for various bath temperatures are shown in Fig. 2.

Although the formula in Eq. (12) was derived for large L_- and large β , it is pragmatically valid down to L_- of order unity and up to (pretty warm) bath temperatures comparable to four times the barrier height. Note that at very high bath temperature ($\beta = 0.05$ in Fig. 2) the transition temperature lies below the bath temperature, a phenomenon known as the inverse Mpemba effect [9]. In the End Matter, we show a behavior that is completely similar to that of yet another potential. We now propose a physical picture rationalizing our findings.

The starting point of our interpretation is a rewriting of Eq. (7)

$$\frac{\partial a_2}{\partial \beta_i} = \int \partial_x \ell_2(x) \Delta U_i(x) dx, \quad (13)$$

where $\Delta U_i(x) = \int_{-\infty}^x dy (V(y) - U_i) \pi(y, \beta_i)$. By the Sturm-Liouville theory, the function $\ell_2(x)$ possesses exactly one zero and is monotonic (we choose $\partial_x \ell_2(x) < 0$). For all practical purposes (see Fig 4 in the End Matter), $\partial_x \ell_2(x) \simeq -\delta(x - x^*)$, so that the only ingredient that matters is the sign of $\Delta U_i(x^*)$ as a function of β_i (the reasoning holds as long as the width of $\partial_x \ell_2(x)$ is smaller than the distance to the wells or walls). We must now understand the thermodynamics of $\Delta U_i(x^*)$ as a function of T_i .

We find it convenient to work directly at $L_+ = +\infty$ initially. At very low temperature T_i , most of the $\pi(x, \beta_i)$ population lies in the deepest minimum where $U_i \simeq \min V$, so that $\Delta U_i(x^*) > 0$ (for $y < x^*$, $V(y) > U_i$). This quantity will remain positive if we slightly increase the temperature, as the Boltzmann distribution starts filling the shallow well, even though U_i increases. Then we consider a much higher temperature T_i so that the Boltzmann distribution now feels the left wall. The distribution lowers and flattens, and begins to extend into the right wing. The contribution of V (bounded to the left) is eventually overtaken by U_i (which grows without bound to infinity as $T_i \rightarrow \infty$), making $\Delta U_i(x^*)$ negative. In terms of population, since $\Delta U_i(x^*) = T_i^2 \partial p_- / \partial T_i$, we see that as T_i increases, what causes the Mpemba effect is the transfer of the probability in the left side to the right one where it can expand (without such a wall to the left, the population would keep increasing on that side, hence killing the Mpemba effect). Now, let us insert a hard boundary to the right of the deepest well. If the latter is placed too close to the minimum, the Boltzmann population reversal cannot occur, and a_2 is monotonic. Still, if, on the contrary, it is placed sufficiently far from the well, in such a way that, as T_i increases, the Boltzmann distribution can sample the population in the vicinity of the left wall beforehand, then there must exist a Mpemba effect.

This analysis of the effect of a wall to the right, which is consistent with Eq. (11), can also be explored numerically, as shown in Fig. 3 for a quartic potential. Finally,

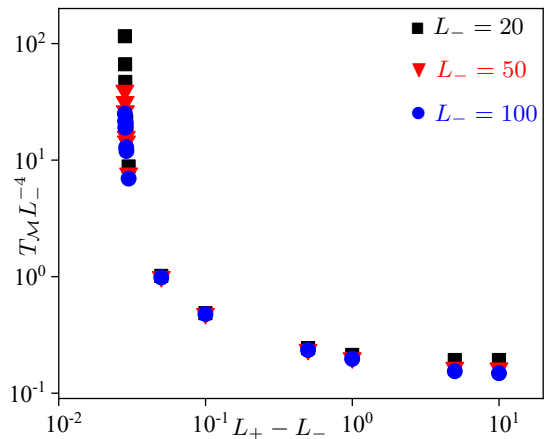


FIG. 3. The temperature $T_{\mathcal{M}}$ is shown as a function of $L_+ - L_-$ for $L_- = 20$ (black), $L_- = 50$ (red) and $L_- = 100$ (blue) when the bath is at $\beta = 10$. The transition temperature $T_{\mathcal{M}}$ diverges as the right wall gets close enough to the left wall, signaling the disappearance of the Mpemba effect. Our prediction Eq. (11) is consistent with the behavior away from $L_+ \simeq L_-$.

if Pandora's box of mathematical possibilities is open to non-analytic potentials, with asymptotic behavior differing to the right and to the left, then of course a hard wall is not a necessary condition. All that is required to observe the Mpemba effect is a steeper potential to the left than to the right. One can even artificially create two transition temperatures (a mathematical curiosity illustrated in the End Matter) by inserting a wall to the right. If anything, this confirms that the Mpemba effect is driven by the asymptotics of the potential regardless of its inner structure, in line with our main message.

In this work, we have considered an asymmetric double-well potential that allows for the existence of a long timescale over which the Mpemba effect could be observed. We have found that the existence of a wall to the left of the shallow well is a necessary condition for the Mpemba effect to occur. The corresponding physics ignores the double-well structure and instead relies on the asymmetry of a coarse-grained one-well potential. If the asymmetry is soft on the left and hard on the right, then the effect is observed. We have also shown that introducing a wall to the right can be sufficient to destroy the Mpemba effect. Our findings now call for a quantitative systematic study [53] of single- and double-well potentials, including cases in symmetric double-well potential and in more than one space dimension without walls [62], and situations where a_2 may not be sufficient (symmetric double-well, *etc.*). Since we claim that the Mpemba effect observed in experiments [4, 52] is wall-driven rather than metastability-induced, it would be very interesting to conduct new experiments to probe the importance of the high-energy shape of the optical trap. What matters

for experimental walls is a steeper divergence than within the branches of the potential landscape.

Acknowledgements. In the course of this work, we have been made aware of a similar endeavor by John Bechhoefer and Siddharth Sane, with whom we had several useful exchanges that helped us clarify our message. We also thank Marija Vucelja and Apurba Biswas for several discussions. H.H. thanks Satoshi Takada for fruitful discussions, and was supported by JSPS KAKENHI Grant No. 26K06960. Y.L. gratefully acknowledges the Yukawa Research Fellow, co-sponsored by the YITP and the Yukawa Memorial Foundation. T.V.V. was supported by JSPS KAKENHI Grants No. JP23K13032 and No. JP26K00022. FvW acknowledges the financial support of the ANR grant THEMA No. 20-CE30-0031-01.

-
- [1] E. B. Mpemba and D. G. Osborne, Cool?, *Phys. Educ.* **4**, 172 (1969).
- [2] H. C. Burridge and P. F. Linden, Questioning the Mpemba effect: Hot water does not cool more quickly than cold, *Sci. Rep.* **6**, 1 (2016).
- [3] J. I. Katz, Reply to Burridge & Linden: Hot water may freeze sooner than cold, *arXiv preprint arXiv:1701.03219* (2017).
- [4] A. Kumar and J. Bechhoefer, Exponentially faster cooling in a colloidal system, *Nature* **584**, 64 (2020).
- [5] R. Chétrite, A. Kumar, and J. Bechhoefer, The metastable Mpemba effect corresponds to a non-monotonic temperature dependence of extractable work, *Front. Phys.* **9**, 654271 (2021).
- [6] A. Kumar, R. Chétrite, and J. Bechhoefer, Anomalous heating in a colloidal system, *Proc. Natl. Acad. Sci. U.S.A.* **119**, e2118484119 (2022).
- [7] A. Biswas, R. Rajesh, and A. Pal, Mpemba effect in a Langevin system: Population statistics, metastability, and other exact results, *J. Chem. Phys.* **159**, 044120 (2023).
- [8] G. Teza, R. Yaacoby, and O. Raz, Relaxation Shortcuts through Boundary Coupling, *Phys. Rev. Lett.* **131**, 017101 (2023).
- [9] Z. Lu and O. Raz, Nonequilibrium thermodynamics of the Markovian Mpemba effect and its inverse, *Proc. Natl. Acad. Sci. U.S.A.* **114**, 5083 (2017).
- [10] A. Lasanta, F. Vega Reyes, A. Prados, and A. Santos, When the Hotter Cools More Quickly: Mpemba Effect in Granular Fluids, *Phys. Rev. Lett.* **119**, 148001 (2017).
- [11] I. Klich, O. Raz, O. Hirschberg, and M. Vucelja, Mpemba index and anomalous relaxation, *Phys. Rev. X* **9**, 021060 (2019).
- [12] M. Baity-Jesi, E. Calore, A. Cruz, L. A. Fernandez, J. M. Gil-Narvi3n, A. Gordillo-Guerrero, D. Iñiguez, A. Lasanta, A. Maiorano, E. Marinari, V. Martin-Mayor, J. Moreno-Gordo, A. Muñoz Sudupe, D. Navarro, G. Parisi, S. Perez-Gavero, F. Ricci-Tersenghi, J. J. Ruiz-Lorenzo, S. F. Schifano, B. Seoane, A. Taranc3n, R. Tripiccion, and D. Yllanes, The Mpemba effect in spin glasses is a persistent memory effect, *Proc. Natl. Acad. Sci. U.S.A.* **116**, 15350 (2019).
- [13] E. Momp3, M. A. L3pez-Castaño, A. Lasanta, F. Vega Reyes, and A. Torrente, Memory effects in a gas of viscoelastic particles, *Phys. Fluids* **33**, 062005 (2021).
- [14] A. Biswas, V. V. Prasad, O. Raz, and R. Rajesh, Mpemba effect in driven granular Maxwell gases, *Phys. Rev. E* **102**, 012906 (2020).
- [15] Z.-Y. Yang and J.-X. Hou, Non-Markovian Mpemba effect in mean-field systems, *Phys. Rev. E* **101**, 052106 (2020).
- [16] R. G3mez Gonz3lez, N. Khalil, and V. Garz3, Mpemba-like effect in driven binary mixtures, *Phys. Fluids* **33**, 053301 (2021).
- [17] A. Biswas, V. V. Prasad, and R. Rajesh, Mpemba effect in an anisotropically driven granular gas, *Europhys. Lett.* **136**, 46001 (2022).
- [18] S. Takada, H. Hayakawa, and A. Santos, Mpemba effect in inertial suspensions, *Phys. Rev. E* **103**, 032901 (2021).
- [19] M. R. Walker and M. Vucelja, Anomalous thermal relaxation of Langevin particles in a piecewise-constant potential, *J. Stat. Mech.* **2021**, 113105 (2021).
- [20] D. M. Busiello, D. Gupta, and A. Maritan, Inducing and optimizing Markovian Mpemba effect with stochastic reset, *New J. Phys.* **23**, 103012 (2021).
- [21] R. Holtzman and O. Raz, Landau theory for the Mpemba effect through phase transitions, *Commun. Phys.* **5**, 280 (2022).
- [22] G. Teza, R. Yaacoby, and O. Raz, Eigenvalue Crossing as a Phase Transition in Relaxation Dynamics, *Phys. Rev. Lett.* **130**, 207103 (2023).
- [23] A. Biswas, V. V. Prasad, and R. Rajesh, Mpemba effect in driven granular gases: Role of distance measures, *Phys. Rev. E* **108**, 024902 (2023).
- [24] A. Biswas and R. Rajesh, Mpemba effect for a brownian particle trapped in a single well potential, *Phys. Rev. E* **108**, 024131 (2023).
- [25] A. Biswas and A. Pal, Mpemba effect on nonequilibrium active Markov chains, *Phys. Rev. E* **111**, 054136 (2025).
- [26] A. Santos, Mpemba meets Newton: Exploring the Mpemba and Kovacs effects in the time-delayed cooling law, *Phys. Rev. E* **109**, 044149 (2024).
- [27] N. Ohga, H. Hayakawa, and S. Ito, Microscopic theory of Mpemba effects and a no-Mpemba theorem for monotone many-body systems, *arXiv preprint arXiv:2410.06623* (2024).
- [28] T. Van Vu and H. Hayakawa, Thermomajorization Mpemba Effect, *Phys. Rev. Lett.* **134**, 107101 (2025).
- [29] A. Nava and R. Egger, Pontus-Mpemba Effects, *Phys. Rev. Lett.* **135**, 140404 (2025).
- [30] A. Nava, R. Egger, B. Dey, and D. Giuliano, Speeding up Pontus-Mpemba effects via dynamical phase transitions, *Phys. Rev. Res.* **7**, 043332 (2025).
- [31] G. Teza, J. Bechhoefer, A. Lasanta, O. Raz, and M. Vucelja, Speedups in nonequilibrium thermal relaxation: Mpemba and related effects, *Phys. Rep.* **1164**, 1 (2026).
- [32] F. Carollo, A. Lasanta, and I. Lesanovsky, Exponentially Accelerated Approach to Stationarity in Markovian Open Quantum Systems through the Mpemba Effect, *Phys. Rev. Lett.* **127**, 060401 (2021).
- [33] F. Ares, S. Murciano, and P. Calabrese, Entanglement asymmetry as a probe of symmetry breaking, *Nat. Commun.* **14**, 2036 (2023).
- [34] A. K. Chatterjee, S. Takada, and H. Hayakawa, Quantum Mpemba Effect in a Quantum Dot with Reservoirs, *Phys.*

- Rev. Lett.* **131**, 080402 (2023).
- [35] A. K. Chatterjee, S. Takada, and H. Hayakawa, Multiple quantum Mpemba effect: Exceptional points and oscillations, *Phys. Rev. A* **110**, 022213 (2024).
- [36] C. Rylands, K. Klobas, F. Ares, P. Calabrese, S. Murciano, and B. Bertini, Microscopic Origin of the Quantum Mpemba Effect in Integrable Systems, *Phys. Rev. Lett.* **133**, 010401 (2024).
- [37] M. Moroder, O. Culhane, K. Zawadzki, and J. Goold, Thermodynamics of the Quantum Mpemba Effect, *Phys. Rev. Lett.* **133**, 140404 (2024).
- [38] S. Yamashika, F. Ares, and P. Calabrese, Entanglement asymmetry and quantum Mpemba effect in two-dimensional free-fermion systems, *Phys. Rev. B* **110**, 085126 (2024).
- [39] S. Liu, H.-K. Zhang, S. Yin, and S.-X. Zhang, Symmetry Restoration and Quantum Mpemba Effect in Symmetric Random Circuits, *Phys. Rev. Lett.* **133**, 140405 (2024).
- [40] X. Wang and J. Wang, Mpemba effects in nonequilibrium open quantum systems, *Phys. Rev. Res.* **6**, 033330 (2024).
- [41] A. Nava and R. Egger, Mpemba Effects in Open Nonequilibrium Quantum Systems, *Phys. Rev. Lett.* **133**, 136302 (2024).
- [42] S. Longhi, Bosonic Mpemba effect with non-classical states of light, *APL Quantum* **1**, 046110 (2024).
- [43] L. K. Joshi, J. Franke, A. Rath, F. Ares, S. Murciano, F. Kranzl, R. Blatt, P. Zoller, B. Vermersch, P. Calabrese, C. F. Roos, and M. K. Joshi, Observing the Quantum Mpemba Effect in Quantum Simulations, *Phys. Rev. Lett.* **133**, 010402 (2024).
- [44] S. A. Shapira, Y. Shapira, J. Markov, G. Teza, N. Akerman, O. Raz, and R. Ozeri, Inverse Mpemba Effect Demonstrated on a Single Trapped Ion Qubit, *Phys. Rev. Lett.* **133**, 010403 (2024).
- [45] J. Zhang, G. Xia, C.-W. Wu, T. Chen, Q. Zhang, Y. Xie, W.-B. Su, W. Wu, C.-W. Qiu, P.-X. Chen, W. Li, H. Jing, and Y.-L. Zhou, Observation of quantum strong Mpemba effect, *Nat. Commun.* **16**, 301 (2025).
- [46] S. Yamashika, P. Calabrese, and F. Ares, Quenching from superfluid to free bosons in two dimensions: Entanglement, symmetries, and the quantum Mpemba effect, *Phys. Rev. A* **111**, 043304 (2025).
- [47] D. J. Strachan, A. Purkayastha, and S. R. Clark, Non-Markovian Quantum Mpemba Effect, *Phys. Rev. Lett.* **134**, 220403 (2025).
- [48] X. Turkeshi, P. Calabrese, and A. De Luca, Quantum Mpemba Effect in Random Circuits, *Phys. Rev. Lett.* **135**, 040403 (2025).
- [49] R. Bao and Z. Hou, Accelerating Quantum Relaxation via Temporary Reset: A Mpemba-Inspired Approach, *Phys. Rev. Lett.* **135**, 150403 (2025).
- [50] N. Beato and G. Teza, Relaxation Control of Open Quantum Systems, *Phys. Rev. Lett.* **136**, 070401 (2026).
- [51] S. Yamashika and F. Ares, Quantum Mpemba Effect in Long-Range Spin Systems, *Phys. Rev. Lett.* **136**, 090402 (2026).
- [52] Y. Tian, Y. Zheng, L.-H. Liu, L. Wang, G.-C. Guo, and F.-W. Sun, Experimental study of Mpemba effect in an energy Langevin system, *Phys. Rev. Res.* **7**, L042020 (2025).
- [53] Y. Liu, T. Van Vu, R. Chétrite, F. van Wijland, and H. Hayakawa, The classical Mpemba effect is boundary-driven (2026).
- [54] J. Bechhoefer, A. Kumar, and R. Chétrite, A fresh understanding of the Mpemba effect, *Nat. Rev. Phys.* **3**, 534 (2021).
- [55] M. Mörsch, H. Risken, and H. D. Vollmer, One-dimensional diffusion in soluble model potentials, *Z. Phys. B - Condens. Matter* **32**, 245 (1979).
- [56] H. Risken, *The Fokker-Planck Equation*, 2nd ed. (Springer, 1996).
- [57] S. Arrhenius, Über die Dissociationswärme und den Einfluss der Temperatur auf den Dissociationsgrad der Elektrolyte, *Z. Phys. Chem.* **4**, 96 (1889).
- [58] H. A. Kramers, Brownian motion in a field of force and the diffusion model of chemical reactions, *Physica* **7**, 284 (1940).
- [59] M. R. Walker and M. Vucelja, Mpemba effect in terms of mean first passage time, *arXiv preprint arXiv:2212.07496* (2023).
- [60] B. J. Matkowsky and Z. Schuss, The exit problem for randomly perturbed dynamical systems, *SIAM J. Appl. Math.* **33**, 365 (1977).
- [61] A. Bovier, M. Eckhoff, V. Gayrard, and M. Klein, Metastability in reversible diffusion processes I: Sharp asymptotics for capacities and exit times, *J. Eur. Math. Soc.* **6**, 399 (2004).
- [62] H. Hayakawa and S. Takada, Mpemba effect in a two-dimensional bistable potential, *arXiv preprint arXiv:2603.24148* (2026).

End Matter

Behavior of $\ell_2(x)$: The eigenvector ℓ_2 of \mathbb{W}^\dagger corresponding to λ_2 is known to have a single node. When λ_2 is quasi-degenerate with 0, which occurs at sufficiently low bath temperature, it takes the form of a step function with a smooth error-function profile; hence, its derivative is a sharply peaked function near the location of the potential barrier. We have plotted in Fig. 4 for various values of β the function $\partial_x \ell_2(x)$ (normalized by the area under the peak $\int_{-\infty}^{+\infty} \partial_y \ell_2(y) dy$). The potential we used is $V(x) = (x^2 - 1)^2 - 0.2x$ (the wells are a distance unity from the center and the top of the barrier, and the potential barrier is also of order unity, hence $\beta = 1$ refers to a temperature of the same order as the central barrier).

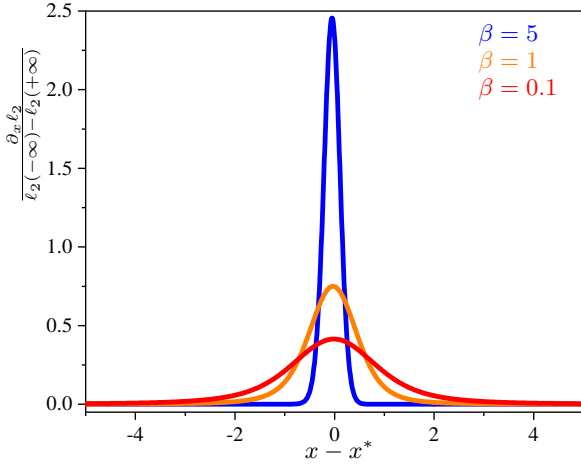


FIG. 4. The function $\partial_x \ell_2$ exhibits a sharp peak at low bath temperature that is robust in the high temperature regime. Regardless of the temperature, it is flatly structureless far from the barrier.

Derivation of Eqs. (10) and (11): Due to Eq. (7), the temperature $T_{\mathcal{M}} = \beta_{\mathcal{M}}^{-1}$, if it exists, is given by

$$\langle \ell_2(x) V(x) \rangle_{\beta_{\mathcal{M}}} - \langle \ell_2(x) \rangle \langle V(x) \rangle_{\beta_{\mathcal{M}}} = 0. \quad (14)$$

At low bath temperature (with an exponentially small error in β), we use $\ell_2(x) \simeq \theta(x - x^*)$, hence

$$U_- p_- - p_- (U_- p_- + U_+ p_+) = 0, \quad (15)$$

where U_{\pm} and p_{\pm} are defined by

$$\begin{aligned} U_{\pm} &:= \pm \frac{1}{p_{\pm}} \int_{x^*}^{\pm\infty} V(x) \pi(x, \beta_i) dx, \\ p_{\pm} &:= \pm \int_{x^*}^{\pm\infty} \pi(x, \beta_i) dx, \end{aligned} \quad (16)$$

and by convention, $V(x) = +\infty$ for $x < -L$ and $x > L_+$. Then the transition temperature solves

$$U_- = U_+. \quad (17)$$

The potential we consider can be written as

$$V(x) = (x - x^*)^n + \sum_{k=0}^{n-1} v_k (x - x^*)^k, \quad (18)$$

and it verifies

$$(x - x^*) V'(x) = nV(x) - \sum_{k=0}^{n-1} (n - k) v_k (x - x^*)^k. \quad (19)$$

By using the above identity and an integration by parts in Eq. (16), we can get

$$\begin{aligned} Z(\beta_i) p_- &= (L_- + x^*) e^{-\beta_i V(-L_-)} + \beta_i n U_- Z(\beta_i) p_- \\ &\quad - \beta_i \sum_{k=0}^{n-1} (n - k) v_k \int_{-L_-}^{x^*} (x - x^*)^k e^{-\beta_i V(x)} dx, \end{aligned} \quad (20)$$

and a similar expression holds for p_+ . Thus we obtain

$$\begin{aligned} U_- &= \frac{1}{n\beta_i} + \frac{\sum_{k=0}^{n-1} (n - k) v_k \int_{-L_-}^{x^*} (x - x^*)^k e^{-\beta_i V(x)} dx}{nZ(\beta_i) p_-} \\ &\quad - \frac{(L_- + x^*) e^{-\beta_i V(-L_-)}}{n\beta_i Z(\beta_i) p_-}, \\ U_+ &= \frac{1}{n\beta_i} + \frac{\sum_{k=0}^{n-1} (n - k) v_k \int_{x^*}^{L_+} (x - x^*)^k e^{-\beta_i V(x)} dx}{nZ(\beta_i) p_+} \\ &\quad - \frac{(L_+ - x^*) e^{-\beta_i V(L_+)}}{n\beta_i Z(\beta_i) p_+}. \end{aligned} \quad (21)$$

For large enough L_{\pm} , the condition $U_- = U_+$ leads to

$$\frac{L_- e^{-\beta_{\mathcal{M}} V(-L_-)}}{n\beta_{\mathcal{M}} p_-} - \frac{L_+ e^{-\beta_{\mathcal{M}} V(L_+)}}{n\beta_{\mathcal{M}} p_+} = \sum_{k=0}^{n-1} \frac{n - k}{n} v_k \Delta \langle x^k \rangle, \quad (22)$$

where $\Delta \langle x^k \rangle$ is defined as

$$\Delta \langle x^k \rangle = \langle x^k \rangle_+ - \langle x^k \rangle_- \quad (23)$$

with

$$\langle x^k \rangle_+ = \frac{\int_{x^*}^{\infty} (x - x^*)^k e^{-\beta_{\mathcal{M}} V(x)} dx}{p_+}, \quad (24)$$

$$\langle x^k \rangle_- = \frac{\int_{-L_-}^{x^*} (x - x^*)^k e^{-\beta_{\mathcal{M}} V(x)} dx}{p_-}. \quad (25)$$

Our task now is to determine the order of $\Delta \langle x^k \rangle$. In the following, we discuss the large L_- limit, and we anticipate that the regime of interest is the high-temperature one with small $\beta_{\mathcal{M}}$, yet with $\beta_{\mathcal{M}} V(-L_-) \gg 1$. In this limit, we have

$$p_- \simeq M_0 - \frac{1}{n\beta_{\mathcal{M}} L_-^{n-1}} e^{-\beta_{\mathcal{M}} L_-^n}, \quad (26)$$

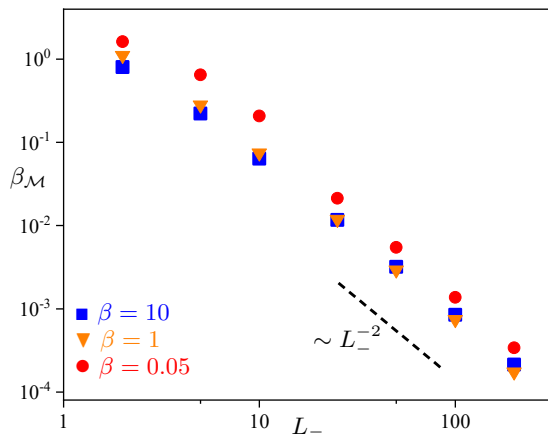


FIG. 5. For a piecewise-quadratic potential, the transition temperature increases quadratically with distance from the wall.

where $M_k = \int_0^\infty x^k e^{-\beta_{\mathcal{M}} x^n} dx$. In addition we see that $M_k \sim \beta_{\mathcal{M}}^{-(k+1)/n}$. For the right and left sides, respectively, we have

$$\langle x^k \rangle_+ \sim \frac{M_k}{M_0}, \quad \langle x^k \rangle_- \sim (-1)^k \frac{M_k}{M_0}. \quad (27)$$

We thus arrive at

$$\Delta \langle x^k \rangle \sim \begin{cases} \beta_i^{-k/n} & \text{for odd } k, \\ 0 & \text{for even } k, \end{cases} \quad (28)$$

which suggests that only the highest odd term $k = k^*$ needs to be considered (this is $k^* = n - 1$ if $v_{n-1} \neq 0$). Therefore, we have

$$\frac{L_- e^{-\beta_{\mathcal{M}} L_-^n}}{n \beta_{\mathcal{M}} \beta_{\mathcal{M}}^{-1/n}} - \frac{L_+ e^{-\beta_{\mathcal{M}} L_+^n}}{n \beta_{\mathcal{M}} \beta_{\mathcal{M}}^{-1/n}} \sim \beta_{\mathcal{M}}^{-k^*/n}, \quad (29)$$

which establishes

$$\beta_{\mathcal{M}} \simeq (n - k^*) \frac{\ln(\text{const } L_-)}{L_-^n} + \frac{1}{L_-^n} \ln \left(1 - \frac{L_+}{L_-} e^{-\beta_{\mathcal{M}} (L_+^n - L_-^n)} \right), \quad (30)$$

irrespective of whether $k^* = n - 1$ or a smaller integer.

Piecewise quadratic potential: Dropping the analyticity hypothesis (*i.e.* than V can be written as a series valid everywhere on the real axis), we construct a piecewise-quadratic potential (continuously differentiable) that attains the weakest possible divergence at infinity (for a discrete spectrum). Our analysis stands and the transition temperature $T_{\mathcal{M}}(L_-)$ behaves as L_-^2 at large L_- , as shown in Fig. 5.

A mathematical curiosity: If the hypothesis to resort to an analytic potential is even more relaxed, then, mostly as a mathematical game, one can artificially construct a potential that not only displays a Mpemba effect without the need for a hard wall (it only takes a steeper divergence), but also exhibits two (or more) transition temperatures. Here, we adopt the choice

$$V(x) = \begin{cases} x^4 - 2x^2 & \text{for } x < 0, \\ \frac{x^4}{1 + ax^2} - 2x^2 & \text{for } x > 0. \end{cases} \quad (31)$$

The left asymptotics x^4 is steeper than the right asymptotics x^2 , which leads to the existence of a Mpemba effect. In addition, if a hard(er) wall is now inserted to the right, a secondary population inversion will occur, and a second transition temperature exists. The numerical illustration of this phenomenon is provided in Fig. 6.

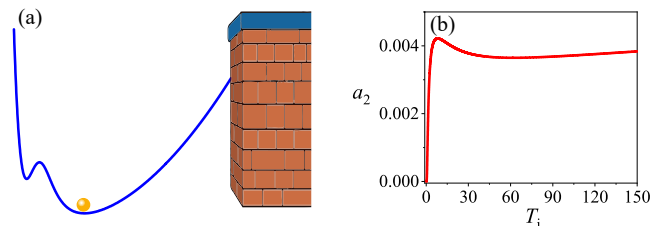


FIG. 6. For the choice $a = 0.49$ in the definition of V in Eq. (31) and $L_+ = 40$, the coefficient a_2 is shown as a function of the initial temperature T_i . This function exhibits extrema.